

→ After you have given an birds-eye-view of why you want to consider CutFEM in general, you can here give a more indepth summary over the concrete approach. ①

4 Cut Continuous Interior Penalty Method for the Biharmonic Problem

Questions arise when we want to allow for complex geometries where some physical domain Ω has a smooth boundary Γ and, thus, cannot be fully covered of a fitted mesh. This motivated us to define a unfitted finite element method.

Computational domain

4.1 Unfitted Mesh *we talk about unfitted now & $\Omega \neq T_h$.*

Let $\Omega \subseteq \mathbb{R}^d$ be a physical domain and Γ be a sufficiently smooth boundary in C^2 .

We want to make a CutFEM version of the CIP problem. Let \tilde{T}_h be a shape-regular and quasi-uniform background mesh. Let us denote the active set $T_h \subseteq \tilde{T}_h$ which intersects the interior of the active domain Ω , that is

$$T_h = \{T \in \tilde{T}_h \mid T \cap \Omega \neq \emptyset\}. \quad \begin{matrix} \text{which covers } \Omega \text{ but which does not} \\ \text{need to fit the domain.} \end{matrix}$$

+ We define with the corresponding set of interior facets. (When you introduce Ω , assume that it is open and bounded.)

$$\mathcal{F}_h^{\text{int}} = \{F = T^+ \cap T^- \mid T^+, T^- \in T_h\},$$

and a set of cut elements "cut by the boundary"

$$\mathcal{T}_\Gamma = \{T \in T_h \mid T \cap \Gamma \neq \emptyset\}. \quad \begin{matrix} \mathcal{T}_\Gamma \\ \mathcal{F}_h^\Gamma \end{matrix}$$

For convenience, will we define also the interior of the active set as T_{int} be consistent, while

$$T_{\text{int}} = \{T \in T_h \mid T \cap \text{Int}(\Omega) \neq \emptyset\}. \quad \begin{matrix} \text{Int} \\ \mathcal{T}_h \quad \mathcal{T}_\Gamma \end{matrix}$$

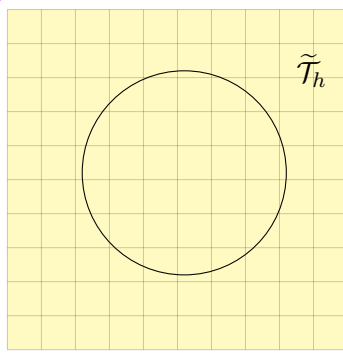
Hence, we have that the active set is the union of the interior and cut elements, $T_h = T_{\text{int}} \cup \mathcal{T}_\Gamma$. For an illustration, see Figure 11.

*Declare operator
later command.*

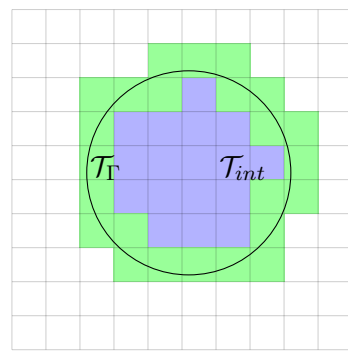
4.2 Cut Continuous Interior Penalty Method

This makes it natural to redefine the biharmonic problem on a unfitted domain. Let $\Omega \subseteq \mathbb{R}^d$ s.t. Γ be its corresponding boundary in C^2 . Then is the BH problem on the form,

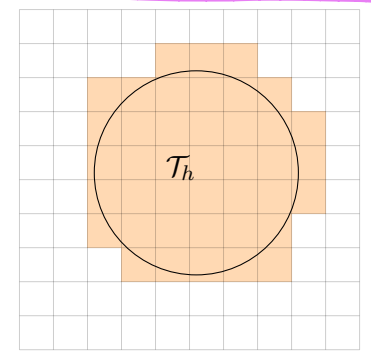
$$\begin{aligned} \Delta^2 u + \alpha u &= f(x) && \text{in } \Omega, \\ \partial_n u &= g_1(x) && \text{on } \Gamma, \\ \partial_n \Delta u &= g_2(x) && \text{on } \Gamma. \end{aligned} \quad (24)$$



(a)



(b)



(c)

Figure 11: Illustration of the background mesh \tilde{T}_h , the active set T_h , the cut cells \mathcal{T}_Γ and the interior of the active set T_{int}

Important: Work on that when we do the overall polishing and the introduction; not how when we're fixing the math

① Describe the general approach, here are some line of thoughts.

- use CIP for BH from Ch 3 as starting point

- A structured / easy-to-generate mesh is introduced.

Will only be used to define approximation spaces, but

does not need to fit the physical domain, so

- Function space is associated with mesh, while

bilinear form is associated with physical domain

- So-called small cut elements where $|T \cap \Omega| \ll |T| \sim h^d$
and $|T \cap T'| \ll h^{d-1}$ prevents us from getting similar
stability / a priori error estimates which are geometrically robust.

Here is $\Delta^2 = \Delta(\Delta)$ the biharmonic operator, also known as the bjlaplacian. We will assume for the strong form that $u \in H^4(\Omega)$, $\alpha > 0$ and $f \in L^2(\Omega)$. For completeness will we also add the corresponding continuous weak formulation. Find a $u \in H^2(\Omega)$ s.t. $a(u, v) = l(v) \forall v \in H^2(\Omega)$ where

$$\begin{aligned} a(u, v) &= (\alpha u, v)_\Omega + (\Delta u, \Delta v)_\Omega + (\partial_n \Delta u, v)_\Gamma - (\partial_n v, \Delta u)_\Gamma - (\partial_n u, \Delta v)_\Gamma \\ l(v) &= (f, v)_\Omega - (g_2, v)_\Omega - (g_1, \Delta v)_\Gamma \end{aligned} \quad (25)$$

Remark. Be aware that the only difference between the strong BH variants, (12) and (24), is that the first one problem is fitted s.t. $\mathcal{T}_h = \Omega$, while the latter is unfitted and equipped with a sufficiently smooth boundary. The continuous weak formulations is entirely identical in its composition.

We denote the C^0 polynomial space of order k as

$$V_h = \left\{ v \in C^0(\Omega) : v_T = v|_T \in \mathcal{P}^k(T), \forall T \in \mathcal{T}_h \right\}$$

Drawing on the principles outlined in Section 3, we can indeed derive two equivalent formulations for the biharmonic equation, specifically adapted to an unfitted mesh. Similarly both formulation is the bilinear form $a_h : V_h \times V_h \rightarrow \mathbb{R}$ and the linear form $l_h : V_h \rightarrow \mathbb{R}$. Recall the recall the Hessian formulation (20) and the Laplace formulation (22) on a polygonal mesh. Then we have the following unfitted variants.

- 1) Assume $g_1(x) = 0$. Then unfitted Hessian formulation has the bilinear form

$$\begin{aligned} a_h^H(u, v) &= (\alpha u, v)_{\mathcal{T}_h \cap \Omega} + (D^2 u, D^2 v)_{\mathcal{T}_h \cap \Omega} \\ &\quad - (\{\partial_{nn} u\}, [\partial_n v])_{\mathcal{F}_h \cap \Omega} - (\{\partial_{nn} v\}, [\partial_n u])_{\mathcal{F}_h \cap \Omega} \\ &\quad - (\partial_{nn} u, \partial_n v)_\Gamma - (\partial_{nn} v, \partial_n u)_\Gamma \\ &\quad + \frac{\gamma}{h} ([\partial_n u], [\partial_n v])_{\mathcal{F}_h \cap \Omega} + \frac{\gamma}{h} (\partial_n u, \partial_n v)_\Gamma \\ l_h^H(v) &= (f, v)_{\mathcal{T}_h \cap \Omega} - (g_2, v) \end{aligned} \quad (26)$$

- 2) The unfitted Laplace formulation has the bilinear form

$$\begin{aligned} a_h^L(u, v) &= (\alpha u, v)_\Omega - (\Delta u, \Delta v)_\Omega \\ &\quad - (\{\Delta u\}, [\partial_n v])_{\mathcal{F}_h} - (\{\Delta v\}, [\partial_n u])_{\mathcal{F}_h} + \frac{\gamma}{h} ([\partial_n u], [\partial_n v])_{\mathcal{F}_h} \\ &\quad - (\Delta u, \partial_n v)_\Gamma - (\Delta v, \partial_n u)_\Gamma + \frac{\gamma}{h} (\partial_n u, \partial_n v)_\Gamma \\ l_h^L(v) &= (f, v)_\Omega - (g_2, v)_\Gamma - (g_1, \Delta v)_\Gamma + \frac{\gamma}{h} (g_1, \partial_n v)_\Gamma \end{aligned} \quad (27)$$

We will in this section do a full proof for the Hessian formulation, however, the proofs should not differ to much for the Laplace formulation. For simplification will we use the notation $a_h(u, v) = a_h^H(u, v)$ and $l_h(v) = l_h^H(v)$ for the rest of the stability and convergence analysis.

To make sure the problem is stabilized will we add a hypothetical consistent symmetric bilinear ghost-penalty term $g_h : V_h \times V_h \rightarrow \mathbb{R}$ in addition to our bilinear. That is, we define the discrete problem to find a $u_h \in V_h$ s.t.

$$A_h(u_h, v) := a_h(u_h, v) + g_h(u_h, v) = l_h(v) \quad \forall v \in V_h. \quad (28)$$

Our overall goal is to show what assumptions that is needed for the ghost-penalty method for the discrete problem to be stable and obtain optimal convergence. Once this is fulfilled will we propose a g_h which fulfills these assumptions.

This does
not make
sense, the
strong form
does not know
anything about
the distribution.

1

① For section 4.2. really just state the
the final weak discrete formulations using the Lepage and Hunsaker
formulations, including the additional ghost stability
Don't repeat things or spend time on things you talked about
before, only write about things which are different now.
So main focus should be on ghost penalty and a high level
motivation on why we need it.

Keep in mind that in contrast to the standard CIP methods, this method is defined on an unfitted mesh. As we will see, the analysis is the ghost penalty a method to ensure numerical stability on cut cell \mathcal{T}_Γ . The main reason why this numerical instability is happening for a unfitted mesh is that when a cell is badly cut, see examples in Figure 12. In other words, when a cell is "badly cut," it means that it is intersected by the boundary Γ in such a way that only a very small part of the cell lies inside or outside the domain. This can lead to a very poor condition number of the local system matrix corresponding to such a cell, causing numerical instability.

The ghost penalty stabilization technique is designed to tackle this issue. Essentially, this approach introduces additional terms into the finite element method that penalize jumps in the discrete solution and its gradients across cell interfaces, typically the cut-cells. This penalty not only improves the conditioning of the system matrix but also enhances the robustness of the method with respect to the location of the boundary inside each cell. However, to make this possible, we assume a so-called fat-intersection property, which will be relevant in Section 4.5.

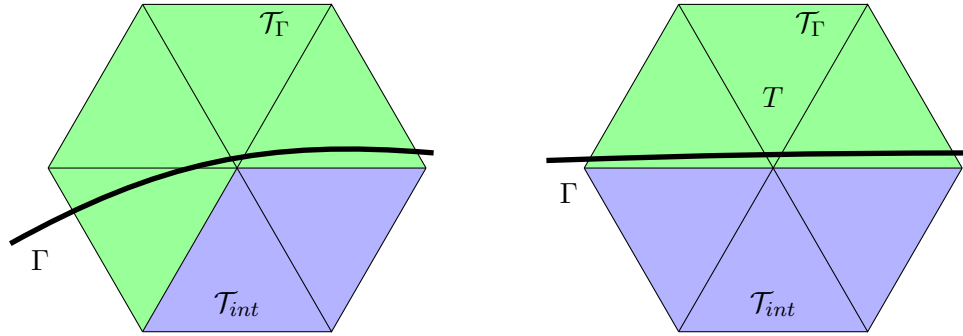


Figure 12: Two examples of bad cut cells. At some point it is even hard to distinguish between interior and cut cells.

We define the underlying norms for $v \in V_h$ as

$$\|v\|_{a_h}^2 = \|\alpha|^{\frac{1}{2}} v\|_{\mathcal{T}_h \cap \Omega}^2 + \|D^2 v\|_{\mathcal{T}_h \cap \Omega}^2 + \gamma \|h^{-\frac{1}{2}} [\partial_n v]\|_{\mathcal{F}_h \cap \Omega}^2 + \gamma \|h^{-\frac{1}{2}} \partial_n v\|_\Gamma^2, \quad (29)$$

$$|v|_{g_h}^2 = g(v, v) \quad (30)$$

$$\|v\|_{A_h}^2 = \|v\|_{a_h}^2 + |v|_{g_h}^2 \quad (31)$$

$$(32)$$

and for $v \in V + V_h$ we get,

$$\|v\|_{a_h,*}^2 = \|v\|_{a_h}^2 + \|h^{\frac{1}{2}} \{\partial_{nn} v\}\|_{\mathcal{F}_h \cap \Omega}^2 + \|h^{\frac{1}{2}} \partial_{nn} v\|_\Gamma^2$$

$$\|v\|_{A_h,*}^2 = \|v\|_{a_h,*}^2 + |v|_{g_h}^2$$

Remark. Note that it holds that $\mathcal{T}_h \cap \Omega = \Omega$ and $\mathcal{T}_h \cap \Gamma = \Gamma$. Depending on context, we choose the best suitable notation.

Remark. As the author knows the exact Laplace formulation (27) with nonhomogeneous boundary conditions, $g_1 \neq 0$, is not found in the literature except for a complete DG formulation presented in [61]. It is expected to have the same well-posedness and convergence properties as the Hessian formulation, hence, in this thesis will we focus on the Hessian formulation for the analysis. In the numerical validation will both methods be presented.

① date (during polishing)

4.3 Stability estimate

Similarly for the Poisson problem will we have the following assumptions for the computational mesh;

- Don't put so much focus on them by putting them into bullet points*
- S.1 Boundary Γ is of C^2 is smooth for simplicity, we gain in assuming C^2 instead
- S.2 The mesh \mathcal{T}_h is quasi-uniform.
- S.3 For a $T \in \mathcal{T}_\Gamma$ there always exists a patch $\omega(T)$ which contains T and an element T' with a so-called fat intersection $|T' \cap \Omega|_d \gtrsim |T'|_d$, where $|\cdot|_d$ is the measure of an element of dimensions $d = 2, 3$. For an illustration, see Figure 13.

① you simply state first time you introduce biharmonic problems

②. you simply mention when you introduce the unfitted background mesh in 4.1.

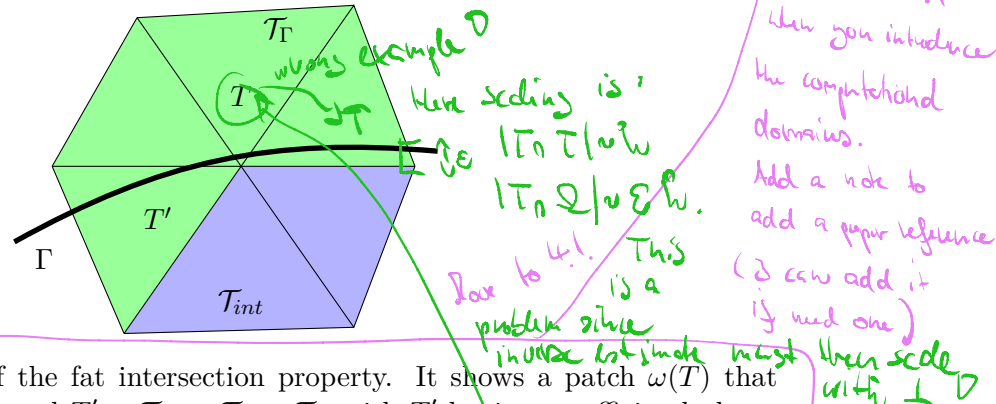


Figure 13: Illustration of the fat intersection property. It shows a patch $\omega(T)$ that contains elements $T \in \mathcal{T}_\Gamma$ and $T' \in \mathcal{T}_{int} \cup \mathcal{T}_\Gamma = \mathcal{T}_h$, with T' having a sufficiently large intersection with Ω .

From basic theory we have the following inverse estimate for $v \in \mathcal{P}^k(T)$ s.t. (2) always white out.

$$\|\partial_{nn} v\|_F \lesssim \|h_T^{-\frac{1}{2}} D^2 v\|_T,$$

where the hidden constant depend on dimension d , order k and the shape regularity. Similarly for cut elements is it easy to see that this must hold,

$$\|\partial_{nn} v\|_{F \cap \Omega} \lesssim \|\partial_{nn} v\|_F \lesssim \|h_T^{-\frac{1}{2}} D^2 v\|_T.$$

A useful variant is the following inequality that is,

$$\|\partial_{nn} v\|_{\Gamma \cap T} \lesssim h^{-\frac{1}{2}} \|D^2 v\|_T.$$

start by explaining that inverse estimate as summarized in section 2. (2) play also a crucial role in the unfitted case, and it is exactly those which become particularly challenging to work with due to the "small cut element" problem

Remark. It may be natural to instead look at $\|\partial_{nn} v\|_{\Gamma \cap T} \lesssim h^{-\frac{1}{2}} \|D^2 v\|_{T \cap \Omega}$, however, this cannot hold for a unfitted mesh. The reason is because it leads to geometric problems when measuring the relationship between the intersected boundary $|\Gamma \cap T|_{d-1}$ and the intersected volume $|T \cap \Omega|$. For the examples provided in Figure 12, we observe that for bad cut configurations the relationship $|\Gamma \cap T|_{d-1} / |T \cap \Omega|_d$ may in fact diverge and, thus, makes it necessary to extend the norm to the full element T for the inequality to hold. (2)

Since the inequalities above holds for all elements locally is it natural to do a global summation over the over \mathcal{F}_h and \mathcal{T}_h . This implies that

$$\|\partial_{nn} v\|_{\mathcal{T}_h \cap \Gamma} \lesssim h^{-\frac{1}{2}} \|D^2 v\|_{\mathcal{T}_h}, \quad (33)$$

$$\|\partial_{nn} v\|_{\mathcal{F}_h \cap \Omega} \lesssim h^{-\frac{1}{2}} \|D^2 v\|_{\mathcal{T}_h}. \quad (34)$$

① Outline main approaches

- abstract g.p. only assumed to be symmetric and positive semi-definite
- additional requirements are derived along the way when you proceed with stability and a priori error analysis.
- Again clearly state your sources, in particular, that you here follow the abstract approach presented for CutDG for Poisson-type problems in [Guerin, Droniou 2019]?

② Description of small cut problem is correct.

First notice that $\|\Gamma \cap T\|_{d-1} / \|\Gamma \cap \Omega\|_d$ always divide to ∞ , even in the filled core,

when $\Gamma \cap \Omega = \emptyset$ and $\|\Gamma\|_{d-1} \sim h^{d-1}$ are $\Gamma \cap \Omega = T$ and $\|\Gamma\|_d \sim h^d$ so $\frac{\|\Gamma\|_{d-1}}{\|\Gamma\|_d} \xrightarrow{h \rightarrow 0} \infty$.

The main problem in the unfilled core is that

$\|\Gamma \cap T\| \sim h^{d-1}$ but $\|\Gamma \cap \Omega\| \sim \varepsilon h^{d-1}$ (and not h^d)

where ε can be arbitrary small.

I've included some pages from my PhD thesis introduction

which explains the problem. There are two cases:

a) "sliver case": when $\|\Gamma \cap T\| \sim h^{d-1}$ but $\|\Gamma \cap \Omega\| \sim \varepsilon h^{d-1}$ $\varepsilon \ll 1$

This is bad for inverse estimates and thus for discrete coercivity.

b) "dollying case" when both $\|\Gamma \cap T\|$ and $\|\Gamma \cap \Omega\| \sim \varepsilon h^{d-1}$

This is bad for conditioning since it means that there are possibly very small (almost vanishing) entries in the system matrix.

3 A gentle introduction to the Nitsche method

As already pointed out, Nitsche's method can be considered as a general methodology for weakly imposing boundary and interface conditions for a wide class of problems. Since the method lies at the core of this thesis, it is worthwhile to explain the basic principles behind the method. These principles can be best exemplified with the Poisson equation as a model problem: Given a domain Ω with boundary $\Gamma = \partial\Omega$, the problem is to find u such that

$$-\Delta u = f \quad \text{in } \Omega, \tag{3.1}$$

subject to the boundary condition

$$u = g \quad \text{on } \Gamma. \tag{3.2}$$

3.1 Boundary conditions

Classically, the Dirichlet boundary (3.2) is strongly imposed by seeking the solution u in some function space V_g consisting of functions which already satisfy (3.2). Nitsche [44] introduced a simple principle where the function space V is not subject to that requirement. Instead, (3.2) is enforced through a weak formulation. To derive the weak form, equation (3.1) is multiplied with a test function v and integrated by parts, giving

$$\int_{\Omega} \nabla u \cdot \nabla v \, dx - \int_{\Gamma} \nabla u \cdot \mathbf{n} v \, dS = \int_{\Omega} f v \, dx. \tag{3.3}$$

Now, the main idea is to weakly enforce the boundary condition (3.2) by penalizing the jump $u - g$:

$$\int_{\Omega} \nabla u \cdot \nabla v \, dx - \int_{\Gamma} \nabla u \cdot \mathbf{n} v \, dS + \gamma \int_{\Gamma} \mu(u - g)v \, dS = \int_{\Omega} f v \, dx. \tag{3.4}$$

where $\gamma > 0$ is a penalty parameter and μ is some “weighting” function to adjust the penalty of the jump. Nitsche [44] proved that the choice $\mu = \gamma h^{-1}$, with h being the local mesh size, gives an optimally convergent method.

Unfortunately, the variational form (3.4) and thus the algebraic system resulting from finite element discretization lacks symmetry. Since symmetry is important for both adjoint consistency of the weak form and for the design of efficient linear solvers, a consistent symmetrization term of the form

$\int_{\Gamma} \nabla v \cdot \mathbf{n}(u - g) dS$ can be added to recover symmetry. The final Nitsche method is then given by the following formulation: find $u \in V$ such that $\forall v \in V$

$$\int_{\Omega} \nabla u \cdot \nabla v dx - \underbrace{\int_{\Gamma} \nabla u \cdot \mathbf{n} v dS}_{\text{Consistency}} - \underbrace{\int_{\Gamma} \nabla v \cdot \mathbf{n} u dS}_{\text{Symmetrization}} + \gamma \underbrace{\int_{\Gamma} h^{-1} uv dS}_{\text{Penalization}} = \quad (3.5)$$

$$\int_{\Omega} f v dx - \underbrace{\int_{\Gamma} \nabla v \cdot \mathbf{n} g dS}_{\text{Symmetrization}} + \gamma \underbrace{\int_{\Gamma} h^{-1} g v dS}_{\text{Penalization}}. \quad (3.6)$$

3.2 Interface conditions

The same guiding principles to weakly imposed boundary conditions via Nitsche's method can be employed to express interface condition by means of variational forms. Again, we consider a model problem based on the Poisson equation (3.1)–(3.2). As shown in Figure 3.1, the domain Ω is now assumed to consist of two subdomains Ω_1 and Ω_2 , separated by the interface $\Gamma = \partial\Omega_1 \cap \partial\Omega_2$.

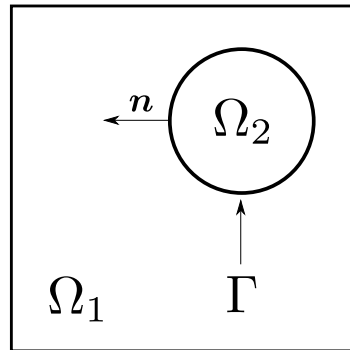


Figure 3.1: Decomposition of the domain Ω by introducing the artificial interface Γ . The weak coupling along the interface Γ by the Nitsche method allows independent meshes for the subdomains Ω_1 and Ω_2 , including overlapping meshes.

A function $v : \Omega \rightarrow \mathbb{R}$ can then be thought of as a composition $v = (v_1, v_2)$, where $v_i = v|_{\Omega_i}, i = 1, 2$ is the restriction of v to each domain. Correspondingly, the original Sobolev space $H^1(\Omega)$ (consisting of functions with weak, square-integrable first order derivatives) might be replaced by a pair of two function

spaces, formally expressed as

$$H^1(\Omega_1) \bigoplus H^1(\Omega_2) = \{(v_1, v_2) : v_1 \in H^1(\Omega), v_2 \in H(\Omega_2)\}. \quad (3.7)$$

The Poisson problem (3.1)–(3.2) can then be recast as an interface problem of the following form: find (u_1, u_2) such that

$$-\Delta u_i = f_i \quad \text{in } \Omega_i, \quad i = 1, 2, \quad (3.8)$$

$$[\nabla u \cdot \mathbf{n}] = 0 \quad \text{on } \Gamma, \quad (3.9)$$

$$[u] = 0 \quad \text{on } \Gamma, \quad (3.10)$$

$$u = 0 \quad \text{on } \partial\Omega, \quad (3.11)$$

where \mathbf{n} is a chosen normal direction, say $\mathbf{n} = \mathbf{n}_2$. Mathematically speaking, the interface conditions (3.9)–(3.10) ensure that the solution parts u_i are compatible along the interface. From a physical point of view, the conditions mean that some quantity of interest and its normal flux is continuous across the interface, for instance a temperature field T and the associated heat flux proportional to $-\nabla T$.

Reusing the idea of penalizing the jump $[u] = u_2 - u_1$ at the interface and adding certain symmetrization terms, the Nitsche-based weak formulation of the interface problem (3.8)–(3.11) reads: find $(u_1, u_2) \in V_1 \bigoplus V_2$ such that

$$a(u, v) = l(v) \quad \forall (v_1, v_2) \in V_1 \bigoplus V_2, \quad (3.12)$$

where

$$\begin{aligned} a(u, v) &= \sum_{i=1,2} \int_{\Omega_i} \nabla u \cdot \nabla v \, dx \\ &\quad - \underbrace{\int_{\Gamma} \langle \nabla u \cdot \mathbf{n} \rangle [v] \, dS}_{\text{Consistency}} - \underbrace{\int_{\Gamma} \langle \nabla v \cdot \mathbf{n} \rangle [u] \, dS}_{\text{Symmetrization}} + \underbrace{\gamma \int_{\Gamma} h^{-1}[u][v] \, dS}_{\text{Penalty/Stabilization}}, \end{aligned} \quad (3.13)$$

$$l(v) = \int_{\Omega} fv \, dx. \quad (3.14)$$

Here, $\langle \nabla u \cdot \mathbf{n} \rangle = \alpha_1 \nabla u_1 \cdot \mathbf{n} + \alpha_2 \nabla u_2 \cdot \mathbf{n}$ with $\alpha_1 + \alpha_2 = 1$ denotes some convex combination of the normal fluxes across the interface.

Despite its striking simplicity of the formulation and the early publication by Nitsche [44], the scheme has not been widely adopted to formulate interface

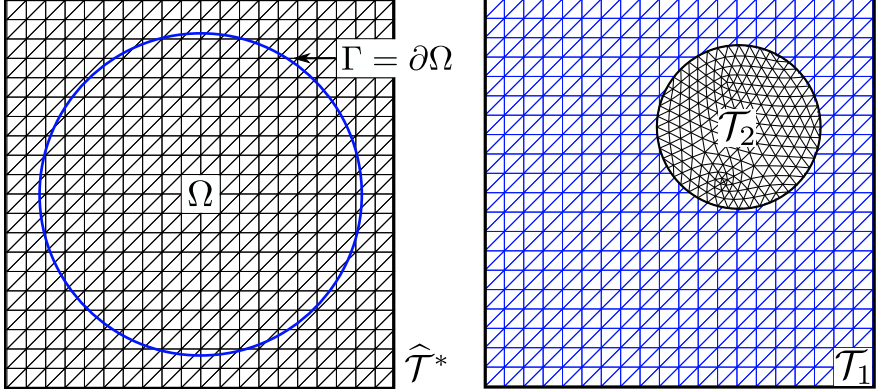


Figure 3.2: Left: Fictitious domain. The discretization of the domain Ω is provided by a larger background mesh. A unfitted surface Γ is given to describe the actual boundary of the physical domain. Right: Overlapping meshes.

problems until fairly recently [8, 35]. Instead, the approach has been first explored in the context of interior penalty or discontinuous Galerkin methods [2, 3], where the finite element functions are discontinuous between *element* interfaces. In a nutshell, certain formulations of the interior penalty based formulations can be interpreted as an element-wise application of the formulation (3.14) to enforce compatibility in a weak sense.

In the introduction, we indicated how an increased flexibility in handling parts of the computational domain independently can be advantageous for certain classes of applications. Now, the Nitsche method can be used to gain this additional flexibility by means of fictitious and overlapping domain formulations. Starting from the weak formulation for boundary and interface conditions presented in this section, the key idea is to simply drop the requirement that the surface Γ needs to be a part of the mesh.

A fictitious domain formulation for the boundary value problem (3.1)–(3.2) is obtained by replacing the mesh for the domain Ω by a larger and possibly easier to generate mesh. This mesh constitutes the fictitious domain. The original physical domain Ω is then described by adding a surface description of the boundary Γ which is now independent of the mesh. See Figure 3.2 for an illustration.

To arrive at an overlapping mesh formulation, the domains Ω_1 and Ω_2 in-

troduced in the previous section are represented by two independent meshes, \mathcal{T}_1 and \mathcal{T}_2 , respectively. In Figure 3.2, the mesh \mathcal{T}_2 is the overlapping mesh, superimposed on a fixed background mesh (\mathcal{T}_0). The remaining portion of the background mesh, not intersected by \mathcal{T}_2 is the mesh \mathcal{T}_1 discretizing Ω_1 .

4 Challenges

Before we turn to a detailed summary of our work in the next section, we devote this section to highlighting some of main challenges encountered in the analysis and implementation of Nitsche-type methods for overlapping and fictitious domains.

As explained in Section 3, the main idea for overlapping and fictitious domain is to replace the mesh-fitted boundary surface and interface by their non-fitted counterparts. As harmless as this step might sound, it has major implications on the analysis and implementation of the resulting schemes.

4.1 Analysis

Broadly speaking, the analysis and algorithmic realization of numerical schemes are usually closely linked to certain stability properties of the schemes. Here, we consider two stability concepts which are important in the context of finite element analysis. The first one is the stability of the bilinear form associated with the weak formulation of the finite element discretization. The second important stability characteristic is the stability, or more commonly the conditioning, of the algebraic system resulting from the finite element discretization.

Following [7], we recall the following stability concepts for the finite element analysis. A bilinear form $A_h : \mathcal{V}_h \times \mathcal{V}_h \rightarrow \mathbb{R}$ defined on some finite element space \mathcal{V}_h is called *weakly coercive* if it for all $u_h \in \mathcal{V}_h$ satisfies

$$\sup_{v_h \in \mathcal{V}} \frac{A_h(u_h, v_h)}{\|v_h\|_{\mathcal{V}_h}} \geq c_A \|u_h\|_{\mathcal{V}_h} \quad (4.1)$$

and it is called *strongly coercive* if

$$A_h(u_h, u_h) \geq c_A \|u_h\|_{\mathcal{V}_h}^2, \quad (4.2)$$

for some fixed constant $c_A > 0$. The weak coercivity of A_h is equivalent to the well-known inf-sup condition

$$\inf_{u_h \in \mathcal{V}_h} \sup_{v_h \in \mathcal{V}_h} \frac{A_h(u_h, v_h)}{\|u_h\|_{\mathcal{V}_h} \|v_h\|_{\mathcal{V}_h}} \geq c_A. \quad (4.3)$$

The conditioning of the algebraic system $\mathcal{A}x = b$ is mainly described by the condition number

$$\kappa(\mathcal{A}) = |\mathcal{A}|_N |\mathcal{A}^{-1}|_N, \quad (4.4)$$

where

$$|\mathcal{A}|_N = \sup_{x \neq 0} \frac{|\mathcal{A}x|_N}{|x|_N}. \quad (4.5)$$

is the operator norm of \mathcal{A} . For linear systems solved by a direct solver, the condition number basically determines the error propagation of input errors. More importantly, when an iterative solver is used, the size of the condition number determines the number of iterations needed to reach a certain prescribed tolerance.

How are these stability properties affected by opting for an unfitted representation of the surface and interface respectively? Roughly speaking, certain scaling properties are lost when simply exchanging a mesh-fitted boundary or interface with their unfitted counterparts. To make the discussion more concrete, we give two examples. For a Nitsche type method, one typical ingredient to prove the stability of the discrete bilinear form, is a so-called inverse inequality of the form

$$\|h^{1/2} \partial_{\mathbf{n}} u\|_{T \cap \Gamma} \leq C \|\nabla u_h\|_{T \cap \Omega}. \quad (4.6)$$

In the fitted case, the boundary part $T \cap \Gamma$ is typically a face F of the element T and $T \cap \Omega = T$ since T belongs to a shape-regular tessellation of Ω . Consequently, there are certain scaling relations between F and T , for instance $h_F |F| \sim |T|$, which in fact allows to prove the inverse inequality (4.6) by means of “scaling arguments”. When the boundary Γ is allowed to cross the element T in an arbitrary manner, the inequality (4.6) is no longer true. Indeed, it can happen that $|T \cap \Omega| \ll |T|$ and $|T \cap \Omega| \ll |T \cap \Gamma|$, as for example in the “sliver case” [13]; see Figure 4.1. To recover the inequality (4.6), one has in fact to incorporate the entire element T into the formulation.

A similar situation occurs in the case of the stability of the linear system $\mathcal{A}x = b$. Here, elements where $|T \cap \Omega| \ll |T|$ and $|T \cap \Gamma| \ll |T|$ lead to an almost vanishing contribution in the stiffness matrix \mathcal{A} . This geometric configuration can be describe as the “dotting case”; see Figure 4.1. If a degree of freedom is associated with only such a type of elements, the matrix \mathcal{A} becomes almost singular [13] and therefore ill-conditioned since the factor $|\mathcal{A}^{-1}|$ in the definition (4.4) of the condition number blows up.

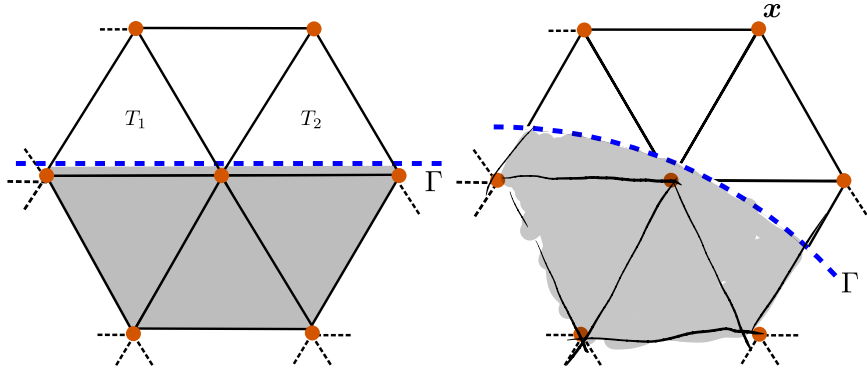


Figure 4.1: Left: Sliver case. Right: Dotting case.

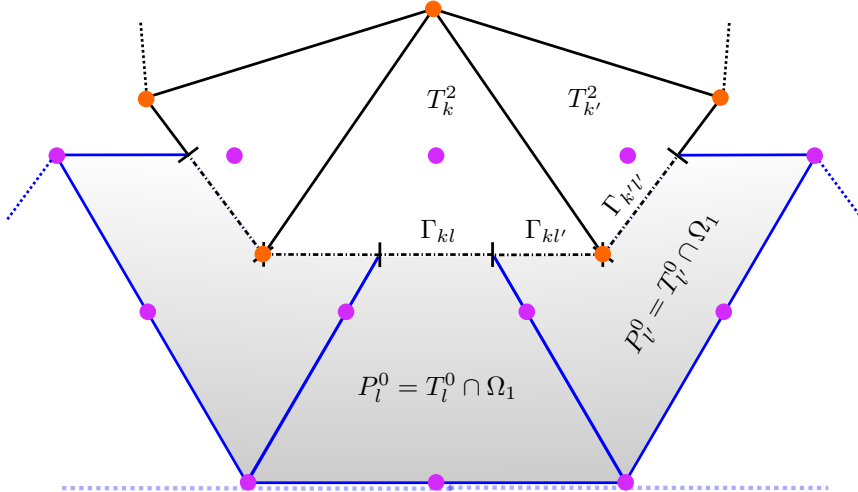


Figure 4.2: The overlapping meshes in the intersection zone. The filled circles represent the degrees of freedom on each element (here for a piecewise linear approximation on \mathcal{T}_2 and piecewise quadratic on \mathcal{T}_0). The interface Γ is partitioned so that each part intersects exactly one cell T_k^2 of the overlapping mesh \mathcal{T}_2 and one cell T_l^0 of the background mesh \mathcal{T}_0 .

4.2 Implementation

We discuss here some of the challenges in realizing a Nitsche overlapped domain method. Similar challenges are encountered in the fictitious domain method.

The main challenges in the implementation of Nitsche's method on overlapping meshes arise from the geometric computations which are necessary to assemble the discrete system associated with (3.13)–(3.14). Naturally, these geometric computations are more involved in 3D than in 2D.

Referring to Figures 3.1 and 4.2, we recall that the situation is the following. The domain Ω_1 is represented by means of a (larger) background mesh \mathcal{T}_0 which is overlapped by a mesh \mathcal{T}_2 , providing a standard tessellation of Ω_2 . Each mesh is associated with a finite element function space. To arrive at the computation of the local element matrices associated with (3.13)–(3.14), a series of preprocessing steps are necessary. First, all cells involved in the intersection between the two meshes have to be found. Since the meshes can overlap arbitrarily and consist of a possibly high number of elements, this is a challenging search problem. Second, a polyhedral representation of the intersected elements depicted in Figure 4.2 has to be provided. Additionally, it is desirable to partition each face on the interface Γ into a set of polygons Γ_{kl} such that Γ_{kl} intersects exactly one element T_k^2 of the overlapping mesh \mathcal{T}_2 and one element T_l^0 of the background mesh \mathcal{T}_0 . The main reason for this procedure is that the interface integrand involves test and trial functions from *different* meshes. Finally, the actual computation of the element integrals arising from (3.13)–(3.14) requires a more complex quadrature procedure, since the uniqueness of each intersected element prevents any sort of quadrature rule precomputation.

5 Summary of papers

5.1 Paper I

In the first paper, we address the key challenges in efficiently implementing finite element methods on overlapping meshes in three space dimension. After reviewing the Nitsche's overlapping mesh formulation and the assembly process for interior penalty methods, three key challenges are identified: the collision detection to find intersections between overlapping meshes, the actual computation of the intersected elements and finally, the integration on complex polyhedra and polygons representing the intersected elements. We address each of these challenges by employing and combining techniques and algorithms from the field of computational geometry. In particular, bounding volume trees are reviewed